

Quantum radiation pressure on a moving mirror at finite temperature

L. A. S. Machado, P. A. Maia Neto, and C. Farina

Instituto de Física, UFRJ, Caixa Postal 68528, 21945-970 Rio de Janeiro, Brazil

(March 21, 2022)

We compute the radiation pressure force on a moving mirror, in the nonrelativistic approximation, assuming the field to be at temperature T : At high temperature, the force has a dissipative component proportional to the mirror velocity, which results from Doppler shift of the reflected thermal photons. In the case of a scalar field, the force has also a dispersive component associated to a mass correction m : In the electromagnetic case, the separate contributions to the mass correction from the two polarizations cancel. We also derive explicit results in the low temperature regime, and present numerical results for the general case. As an application, we compute the dissipation and decoherence rates for a mirror in a harmonic potential well.

I. INTRODUCTION

In his seminal paper published in 1948 [1], Casimir computed the attractive force between two neutral perfectly conducting plates due to vacuum fluctuations of the electromagnetic field. The Casimir force itself is a fluctuating quantity [2], and from the general argument related to the fluctuation-dissipation theorem [3] one may expect that dissipation occurs in the case of moving boundaries. The energy dissipated from macroscopic moving bodies yields for the creation of real particles (photons in the case of the electromagnetic field) [4]. Hence the vacuum radiation pressure on moving boundaries has a dissipative component that plays the role of a radiation reaction force.

This effect takes place even in the case of a single moving plate, as shown by Fulling and Davies [5]. They treated exactly the problem of a massless scalar field in $1+1$ dimensions in the presence of a plate moving in a prescribed arbitrary way. However, since they employed a method based on conformal transformations, their results could not be generalized to higher dimensions. In order to address the case of $3+1$ dimensions in the non-relativistic regime, a convenient perturbative method was proposed by Ford and Vilenkin [6]. Their approach is based on the assumption that the field modulation induced by the motion of the plate is a small perturbation, which is computed up to first order on the displacement of the plate. They considered a massless scalar field, in either $1+1$ or $3+1$ dimensions. In the former case, the dissipative force is proportional to the third time derivative of the plate's displacement, and corresponds to the non-relativistic limit of Fulling and Davies' result. For $3+1$ dimensions the force on a plane mirror moving along the normal direction is proportional to the fifth time derivative of the displacement. This is also the case when the electromagnetic field is considered [7], although the proportionality factor is not simply twice the value found for the scalar case, as would be guessed by crude analogy with the static Casimir effect. Higher order derivatives appear when considering moving mirrors of finite extent [8].

A dissipative force proportional to the velocity of the mirror (like a viscous force) would clearly violate the Lorentz invariance of the vacuum field. For a thermal field, on the other hand, this requirement does not hold, and the thermal contribution to the dissipative force turns out to be proportional to the velocity in the case of $1+1$ dimensions [9]. The effect of thermal photons is larger than the contribution of vacuum fluctuations to the force for temperatures larger than $\hbar\omega_0 = k_B T$ (where k_B is the Boltzmann constant, and ω_0 a typical mechanical frequency). This corresponds to temperatures in the mK range for frequencies in the MHz range. This clearly shows the importance of temperature in the dynamical Casimir effect, which would probably provide the dominant contribution in any attempt to measure the force. Thermal effects on the generation of photons in a cavity with moving mirrors have also been considered [10].

In this paper, we analyze the thermal contributions to the radiation pressure force in $3+1$ dimensions, for both scalar and electromagnetic fields. We take a perfectly-reflecting plane mirror moving along the normal direction, in the non-relativistic regime. Our approach allows us to identify and distinguish between the field modes contributing to the dissipative component of the force from those contributing to its dispersive component. We derive analytical results in the low and high temperature limits, and also compute numerically the force in the general case. The paper is organized as follows: in the next section we take a massless scalar field under Dirichlet boundary condition. In Sec. III, we consider the electromagnetic field. The results of this section are then applied, in Sec. IV, to the analysis of dissipation and decoherence of a mirror in a potential well. Section V presents an interpretation of the results in the high-temperature limit and some concluding remarks.

e-mail: pamn@if.ufrj.br

We choose Cartesian axis such that the plane of the mirror is parallel to the OXY plane. The mirror is displaced along the OZ direction in a prescribed, non-relativistic way. Hence the field satisfies the wave equation and the Dirichlet boundary condition:

$$\partial_z^2 \phi = 0 \quad \text{with} \quad \phi(x, y; q(t); t) = 0; \quad (1)$$

where $q(t)$ denotes the position of the mirror at time t : We assume that $q(t)$ is small when compared with some characteristic field wavelength. We follow the perturbative approach of Ford and Vilenkin [6] and write the field as

$$\phi = \phi^0 + \phi^1; \quad (2)$$

where ϕ^0 is the solution of the corresponding static problem:

$$\partial_z^2 \phi^0 = 0 \quad \text{with} \quad \phi^0(x, y; 0; t) = 0; \quad (3)$$

and ϕ^1 is a small motion-induced perturbation. By taking the Taylor expansion around $z = 0$ up to first order in q ; we derive the following boundary condition:

$$\phi(x, y; 0; t) = q(t) \partial_z \phi^0(x, y; 0; t) + O(q^2); \quad (4)$$

We solve for ϕ in terms of ϕ^0 in the Fourier representation, defined as (using capital letters for Fourier transforms)

$$\phi(z; k_k; !) = \int_{-\infty}^{\infty} dt \int_{-\infty}^{\infty} d^2 r_k e^{i! t} e^{-i k_k \cdot \mathbf{r}} \phi(r_k + z\hat{z}; t); \quad (5)$$

We find

$$\phi(z; k_k; !) = e^{i \mathbf{r} \cdot \mathbf{j}} \int_{-\infty}^{\infty} \frac{d!_{in}}{2} Q(!_{in} - !_0) \phi_z^0(0; k_k; !_{in}); \quad (6)$$

where (we take $c = 1$)

$$Q(!) = [(! + i\epsilon)^2 - k_k^2]^{-1/2} \quad \text{with} \quad \epsilon \rightarrow 0^+$$

is defined, for a given value of k_k , as a function of $!$ with a branch cut along the real axis between k_k and $-k_k$; so that Q is positive for $! > k_k$; negative for $! < -k_k$; and equal to $i \sqrt{k_k^2 - !^2}$ otherwise. Then, when corresponding to a propagating field, Q propagates outwards from the region around the moving mirror; otherwise it corresponds to an evanescent wave. According to (6), the scattering by the moving plate generates frequency modulation: for a given mechanical frequency $!_0$; the input field Fourier component at frequency $!_{in}$ is scattered into a new frequency $! = !_{in} + !_0$: Due to translational symmetry along the OXY plane, all scattered components have the same k_k : If $!_{in} + !_0 < k_k$; the scattered wave is evanescent.

We write the Fourier representation of the unperturbed field in the half-space $z > 0$ in terms of the bosonic operators $a(k)$:

$$\phi^0(z; k_k; !) = i \int_{-\infty}^{\infty} \frac{16^{-3/2} h^{\mathbf{j}} j}{2} \sin(j \cdot \mathbf{r}) a(j \cdot \hat{z} + k_k) (!) + a(j \cdot \hat{z} - k_k)^{\dagger} (-!) (-^2); \quad (7)$$

where θ denotes the step function. This equation shows explicitly the association between positive (negative) frequencies and annihilation (creation) operators. Moreover, the normal mode decomposition includes only propagating waves (since evanescent waves do not satisfy the required boundary condition), hence the factor $(-^2)$: A similar representation may be written for the field in the half-space $z < 0$ in terms of independent bosonic operators $b(k)$ (and their Hermitian conjugates).

We compute the radiation pressure force from the stress tensor component

$$T_{zz} = \frac{1}{2} (\partial_x \phi)^2 + (\partial_y \phi)^2 - (\partial_z \phi)^2 - (\partial_t \phi)^2; \quad (8)$$

taken at the surface of the moving mirror. Up to first order in q ; the force is given by

$$\mathbf{f}(t) = \int_{\Sigma} d\mathbf{x} d\mathbf{y} \left[T_{zz}(\mathbf{x}; \mathbf{y}; 0^+; t) - T_{zz}(\mathbf{x}; \mathbf{y}; 0^-; t) \right] \quad (9)$$

where $\{\mathbf{f}\}_{\pm}$ denoting the anti-commutator

$$T_{zz}(\mathbf{x}; \mathbf{y}; z; t) = \frac{1}{2} \left[\partial_z^2 \phi(\mathbf{x}; \mathbf{y}; z; t); \partial_z^2 \phi(\mathbf{x}; \mathbf{y}; z; t) \right] \quad (10)$$

is the motion-induced modification of the stress tensor. Its Fourier representation may be computed from Eqs. (6) and (10). When taking the average over a given field state we find (with $\mathbf{f} = 0^+$)

$$\langle \text{ht}_{zz}(0^+; \mathbf{k}_k; \mathbf{l}) \rangle_i = \frac{i}{2} \int_{\Sigma} \frac{d\mathbf{l}_1}{2} \int_{\Sigma} \frac{d^2 \mathbf{k}_{1k}}{(2\pi)^2} (\mathbf{l} - \mathbf{l}_1 + i)^2 \left(\mathbf{k}_k - \mathbf{k}_{1k} \right)^{1=2} \frac{d\mathbf{l}_2}{2} Q(\mathbf{l} - \mathbf{l}_1 - \mathbf{l}_2) \langle \mathbf{k}_{1k}; \mathbf{l}_1; \mathbf{k}_k - \mathbf{k}_{1k}; \mathbf{l}_2 \rangle; \quad (11)$$

where

$$\langle \mathbf{l}; \mathbf{l}_2 \rangle = \langle \partial_z^2 \phi(0^+; \mathbf{k}_{1k}; \mathbf{l}_1); \partial_z^2 \phi(0^+; \mathbf{k}_{2k}; \mathbf{l}_2) \rangle \quad (12)$$

is the correlation function of the unperturbed field taken at the OXY plane. For a thermal field, we find, using the normal mode decomposition as given by (7):

$$\langle \mathbf{l}; \mathbf{l}_2 \rangle = 16^{-3} \hbar \frac{\mathbf{l}_1^2 \mathbf{k}_{1k}^2}{\mathbf{l}_1^2 \mathbf{k}_{1k}^2} (\mathbf{l}_1^2 \mathbf{k}_{1k}^2) (\mathbf{l}_1 + \mathbf{l}_2)^{(2)} (\mathbf{k}_{1k} + \mathbf{k}_{2k}) [1 + 2\bar{n}(\mathbf{j}_1, \mathbf{j})] \quad (13)$$

where

$$\bar{n}(\mathbf{j}_1, \mathbf{j}) = (e^{\hbar \mathbf{j}_1 \cdot \mathbf{j} / (k_B T)} - 1)^{-1}$$

is the average photon number at temperature T:

We now analyze in detail the expression in the r.h.s. of Eq. (13). The factor $1 + 2\bar{n}(\mathbf{j}_1, \mathbf{j})$ originates from the general relation between the thermal averages of anti-commutators and commutators, as given by the fluctuation-dissipation theorem [11]. For the field operators themselves, the commutator is a c-number, hence the temperature dependence comes solely from this factor. The factor $^{(2)}(\mathbf{k}_{1k} + \mathbf{k}_{2k})$ is a signature of a homogeneous field state: it means that the correlation function for two given points on the surface of the plate depends only on the relative position between the points. When replaced into (11), it yields for an uniform pressure over the surface of the plate. Likewise, the factor $(\mathbf{l}_1 + \mathbf{l}_2)$ in Eq. (13) is a signature of a stationary field state. When written in the time domain, it corresponds to a correlation function depending only on the time difference, not on the individual times themselves. When replaced in (11), this factor singles out the mechanical Fourier component at the same frequency \mathbf{l} appearing in the argument of $\text{ht}_{zz}(0^+; \mathbf{k}_k; \mathbf{l})$: To compute the force from (9), we also need the motion-induced stress correction at $z = 0^-$; which is computed from (6) and the normal mode decomposition of the field in the half-space $z < 0$ in analogy with the derivation of (11). Its contribution simply doubles the value of the net force, which we write as (we employ the superscript D to denote the results for the scalar field obeying Dirichlet boundary conditions)

$$\mathbf{F}^D(\mathbf{l}) = -^D(\mathbf{l}) - Q(\mathbf{l}); \quad (14)$$

We replace Eq. (13) into Eq. (11) and integrate over the OXY plane to derive the susceptibility function $^D(\mathbf{l})$ (A is the area of the mirror):

$$^D(\mathbf{l}) = \frac{i\hbar A}{2} \int_{\Sigma} d\mathbf{l}_{in} \int_{\Sigma} d\mathbf{k}_k \int_{\Sigma} d\mathbf{l}_j \int_{\Sigma} d\mathbf{l}_j \frac{1=2}{\mathbf{l}_{in}^2 \mathbf{k}_k^2} \frac{1}{2} + \bar{n}(\mathbf{j}_{in}, \mathbf{j}); \quad (15)$$

where we have replaced the variable of integration \mathbf{l}_2 in (11) by \mathbf{l}_{in} ; since it corresponds to the frequency of the unperturbed field ϕ_0 [or input frequency, see Eq. (6)].

The imaginary part of the susceptibility provides, according to Eq. (14), a force component in quadrature with the displacement. If $\text{Im } ^D > 0$; this force component is in opposition of phase with respect to the velocity of the mirror, and hence dissipates its mechanical energy. On the other hand, the real part provides the dispersive force component, which is in quadrature with the velocity, and does not engender any energy exchange when averaging over a sufficiently long time interval. According to Eq. (15), $\text{Re } ^D$ results from contributions of input modes satisfying $|\mathbf{j}| + |\mathbf{l}_{in}| < k_k$; i.e. (propagating) modes that generate evanescent waves when scattered by the mechanical Fourier component \mathbf{l} : In

Fig. 1, we represent the region for the integration in the r.h.s. of (15), corresponding to the condition $j_{\text{in}} j_k \geq 0$ (all input modes are propagating waves), in the plane $\omega_{\text{in}} - k_k$. It is divided in four subsets, labeled R_1 to R_4 [7]. In this diagram, the scattering by the mechanical frequency ω corresponds to a horizontal displacement, by an amount equal to ω , from the point of coordinates $(\omega_{\text{in}}; k_k)$ representing a given input mode (for the sake of clarity we assume $\omega > 0$ in the diagram). The contribution to the dispersive component of the force comes from region R_4 ; the region that occupies the evanescent sector when shifted by ω ; whereas R_1 to R_3 contribute to dissipation.

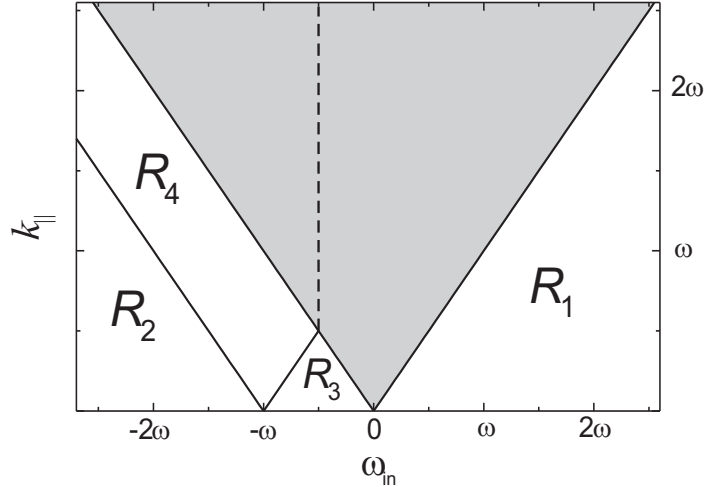


FIG. 1. Diagram for the evaluation of the susceptibility, given by the integrals in the r.h.s. of (15) (scalar or electromagnetic TE-polarized modes) and (23) (electromagnetic TM-polarized modes). Field modes propagating along different directions corresponding to the same values of $k_k = |k_{\text{in}}|$ and frequency are represented by a single point in the $\omega_{\text{in}} - k_k$ plane of integration. Evanescent input modes ($j_{\text{in}} j_k < 0$; grey region) are excluded. Regions R_1 to R_3 yield the dissipative component of the force, whereas region R_4 ; corresponding to input propagating waves that are scattered into evanescent waves, provides the dispersive component. At zero temperature, the contributions from R_1 and R_2 cancel, because the integrand in these regions is anti-symmetric with respect to reflection around the axis at $\omega_{\text{in}} = \omega/2$; which is indicated by a dashed line.

There are two distinct terms in the r.h.s. of (15), both contributing to the dispersive and dissipative components: one proportional to $\bar{n}(j_{\text{in}} j_k)$; corresponding to thermal fluctuations, and one independent of temperature, containing the effect of vacuum fluctuations (with \bar{n} replaced by $1/2$). Accordingly, we write the susceptibility as

$$D = D_T + D_{\text{vac}} :$$

At zero temperature, we have by definition $D_{T=0} = 0$ and $D = D_{\text{vac}}$: It is then particularly useful to consider the reflection around the axis $\omega_{\text{in}} = \omega/2$ (indicated by a dashed line in Fig. 1), which is implemented by the transformation $\omega_{\text{in}} \rightarrow \omega - \omega_{\text{in}}$; while keeping k_k unchanged. The contributions from points in region R_2 cancel exactly those from their conjugates in region R_1 in the integral in Eq. (15). As a consequence, the single contribution to dissipation at zero temperature comes from R_3 ; the only bounded region in the diagram: it corresponds to negative-frequency input modes that are scattered into positive-frequency propagating modes. We evaluate the resulting integral to find

$$\text{Im } D_{\text{vac}}(\omega) = \frac{\hbar A}{360 \pi^2} \omega^5 ; \quad (16)$$

in agreement with Ref. [6]. Thus, the dissipative force exerted by the vacuum field is caused by the motion-induced mixture between positive and negative field frequencies. The discussion following Eq. (7) indicates that this mixture is a signature of a Bogoliubov motion-induced transformation of creation into annihilation operators (and vice-versa), which is clearly connected to the emission of particles [12] [13]. In fact, the dissipative force in vacuum plays the role of a quantum radiation reaction force, dissipating the mechanical energy at exactly the rate required, by energy conservation, for the photon emission effect.

As for the dispersive component of the force, on the other hand, the integral runs over the unbounded region R_4 ; and the vacuum contribution diverges. After regularization, the dispersive force leads to renormalization of the mass of the mirror [6], an effect analyzed in detail for a dielectric interface in Refs. [14] and [15] and for a dispersive mirror in Ref. [16].

We now analyze the thermal contribution to the force, represented by χ_T^D : In contrast with the vacuum force, the thermal dispersive force, as given by the integral over region R_4 , is finite, because the average photon number decreases exponentially to zero at high frequencies. In Appendix A, we show that $\text{Re } \chi_T^D(\omega) < 0$ for any ω (on the other hand, the imaginary part must be positive so as to provide dissipation). The ratio $\chi_T^D/\text{Im } \chi_{\text{vac}}^D$ is a function of a single parameter, $k_B T = (\hbar\omega)$: Numerical results for $\text{Re } \chi_T^D/\text{Im } \chi_{\text{vac}}^D$ are shown in Fig. 2 (dashed line). The dominant contribution comes from input frequencies satisfying $\omega_{\text{in}} \lesssim kT = \hbar\omega$; when $k_B T \ll \hbar\omega$; this condition implies $\omega_{\text{in}} \ll \omega$; and hence the dominant contribution to χ_T^D comes from the close neighborhood of $\omega_{\text{in}} = 0$ in Fig. 1. However, region R_4 is separated from this neighborhood (see Fig. 1), and the larger contribution comes from nearly grazing field modes with frequencies close to $\omega_{\text{in}} = \omega/2$: The corresponding average photon number is $\bar{n} \approx \exp(-\hbar\omega/2kT)$; hence $\text{Re } \chi_T^D$ is exponentially small in this limit. In Appendix A, we derive

$$\text{Re } \chi_T^D(\omega) \approx -\frac{1}{2} \frac{(k_B T)^3}{\hbar^2} A \omega^2 \exp\left(-\frac{\hbar\omega}{2k_B T}\right) \quad (17)$$

Fig. 2 suggests that $\text{Re } \chi_T^D$ grows according to a power law when $k_B T = (\hbar\omega) \gg 1$: Neglecting terms of the order of $(\hbar\omega/k_B T)^2$; we derive in Appendix A the following result for the dispersive thermal susceptibility in the high-temperature limit:

$$\text{Re } \chi_T^D(\omega) \approx -\frac{(3)'}{2} \frac{(k_B T)^3}{\hbar^2} A \omega^2; \quad (18)$$

where $(3)'$ denotes the Riemann zeta function [17].

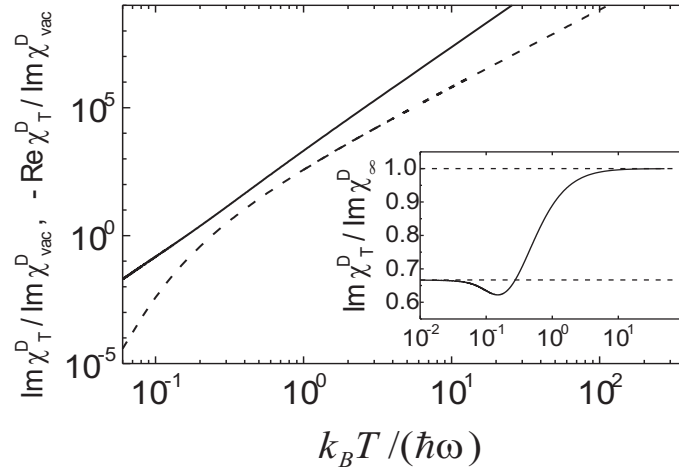


FIG. 2. Thermal susceptibility for the scalar field. The solid line represents $\text{Im } \chi_T^D$; whereas the dashed line represents $-\text{Re } \chi_T^D$; both divided by $\text{Im } \chi_{\text{vac}}^D$: In the insert, we plot $\text{Im } \chi_T^D$ divided by its high-temperature asymptotic value, showing the cross-over between the low and high temperature regimes.

The thermal dissipative susceptibility $\text{Im } \chi_T^D$ is computed from Eq. (15) in a similar way. We define [with $k_B T = (\hbar\omega)$]

$$G^D(\omega) = \frac{\text{Im } \chi_T^D(\omega)}{\text{Im } \chi_{\text{vac}}^D(\omega)} \quad (19)$$

In Appendix B, we derive the results $G^D(\omega) = 24/4$ for $\omega \gg 1$; and $G^D(\omega) = 16/4$ for $\omega \ll 1$: We plot $G^D(\omega)$ in Fig. 2 (solid line), showing that the thermal contribution to dissipation becomes larger than the vacuum effect for $k_B T = (\hbar\omega) > 0.2$: However, the deviation from the high-temperature behavior is not visible in this plot. In the insert of Fig. 2, we plot the ratio $\text{Im } \chi_T^D(\omega)/\text{Im } \chi_{\text{vac}}^D(\omega)$; showing the smooth cross-over between the low and high temperature regimes. A similar cross-over occurs when considering the dissipative susceptibility for the electromagnetic field, as discussed in the next section.

III. ELECTROMAGNETIC FIELD

We consider the following boundary conditions for the electric and magnetic fields E^0 and B^0 measured in the instantaneously co-moving Lorentz frame S^0 :

$$\hat{z} \cdot E^0(x^0; y^0; z^0 = 0) = 0 \quad \hat{z} \cdot B^0(x^0; y^0; z^0 = 0) = 0: \quad (20)$$

We write

$$E(z; k_k; !) = E^{(TE)}(z; k_k; !) + E^{(TM)}(z; k_k; !);$$

where $E^{(TE)}$ is perpendicular to the plane defined by the vectors \hat{z} and k_k ; whereas $E^{(TM)}$ is parallel to this plane. When considering the scattering by the moving plane mirror, these two polarizations are not mixed, and may be mapped into two scalar-field boundary value problems. For TE polarization, Eq. (20) yields a Dirichlet boundary condition for the vector potential in the laboratory frame identical to Eq. (1). The contribution of TE-polarized field modes coincides with the results found for the scalar field in the previous section: $\chi^{(TE)} = \chi^D$:

In order to compute the contribution from TM-polarized modes, we follow the approach of Ref. [7] and define a new vector potential:

$$E^{(TM)} = -\nabla A; \quad B^{(TM)} = \frac{\partial A}{\partial t}: \quad (21)$$

From Eq. (20), we derive a Neumann boundary condition for A in the co-moving frame [18]:

$$\frac{\partial A}{\partial z^0}(x^0; y^0; z^0 = 0) = 0: \quad (22)$$

From this point we proceed as in the previous section. After a lengthy calculation, we find for the contribution of TM-polarized modes

$$\chi^{(TM)} = \frac{i\hbar A}{2} \int_{-\infty}^{\infty} d!_{in} \int_0^{\infty} d k_k k_k \frac{k_k^2 !_{in} (! + !_{in})}{(! + !_{in} + i'')^2 k_k^2 !_{in}^2 k_k^2} \frac{1}{2} + \bar{n}(!_{in}) : \quad (23)$$

The integration region for the evaluation of $\chi^{(TM)}$ is divided as shown in Fig. 1, with R_4 providing its real part, and R_1 to R_3 its imaginary part as in the scalar case. The vacuum contribution was already discussed in detail in Ref. [7]. For the imaginary part, the contributions from regions R_1 and R_2 cancel, and R_3 yields a contribution larger than the TE result, so that the total dissipative susceptibility for the electromagnetic case is not simply twice the result of Eq. (16) for the scalar field:

$$\text{Im} \chi_{vac}^{EM} = \text{Im} \chi_{vac}^{(TE)} + \text{Im} \chi_{vac}^{(TM)} = \frac{\hbar A}{30} !^5: \quad (24)$$

The TM contribution to the real part, on the other hand, cancels the $!^2$ (inertial) term from TE modes, but a $!^4$ divergent term remains [7].

A similar cancelation takes place when considering the thermal contribution in the high-temperature limit. Starting from Eq. (23), we show in Appendix A that $\text{Re} \chi_T^{(TM)}(!)$ is positive for any $!$ (whereas the TE contribution is negative), and derive

$$\text{Re} \chi_{T!1}^{(TM)}(!) = \frac{(3)(k_B T)^3}{2} \frac{A !^2}{h^2}: \quad (25)$$

Thus, the TM contribution cancels the TE contribution as given by (18) to leading order of $k_B T = (\hbar !)$; and the resulting electromagnetic dispersive susceptibility is smaller than the scalar susceptibility by a factor of the order of $(\hbar ! = k_B T)^2$: For finite values of $k_B T = (\hbar !)$; $\text{Re} \chi_T^{(TM)}(!)$ is larger than $\text{Re} \chi_T^{(TE)}(!)$; so that $\text{Re} \chi_T^{EM}(!)$ is always positive. In Fig. 3, we plot $\text{Re} \chi_T^{EM}$ divided by $\text{Re} \chi_{T!1}^D(!)$ as a function of $k_B T = (\hbar !)$; showing the $(k_B T = \hbar !)^{-2}$ behavior at high temperatures.

In the low temperature limit, on the other hand, both contributions become exponentially small. In Appendix A, we find

$$\text{Re } \chi_{T!0}^{\text{TM}}(\omega) = \frac{1}{8} k_B T A \omega^4 \exp \left(-\frac{\hbar \omega}{2k_B T} \right) : \quad (26)$$

The leading contribution to both TE and TM terms originate from field modes propagating close to grazing directions, and with frequencies close to ω_0 . As discussed in Sec. II, the resulting susceptibility is exponentially small because it is proportional to the average photon number at frequency ω_0 . As compared to TE field modes [see (17)], TM modes provide a larger contribution, by a factor of the order of $(\hbar \omega_0 / k_B T)^2$; so that $\text{Re } \chi_{T!0}^{\text{EM}}(\omega) = \text{Re } \chi_{T!0}^{(\text{TM})}(\omega)$. This is in line with the preference for TM polarization when considering propagation along a direction parallel to the plane of the mirror, since it matches the boundary conditions in the static case.

For the imaginary part, we define, in analogy with (19),

$$G^{\text{EM}}(\omega) = \frac{\text{Im } \chi_T^{\text{EM}}(\omega)}{\text{Im } \chi_{\text{vac}}^{\text{D}}(\omega)} : \quad (27)$$

As discussed in Appendix B, TM and TE modes provide identical contributions in the high temperature limit, hence $\text{Im } \chi_T^{\text{EM}}$ is simply twice the value for the scalar field in this limit: $G^{\text{EM}}(\omega) \approx 48 \omega^4$. The TM contribution in the low temperature limit is also analyzed in Appendix B. We find $G^{\text{EM}}(\omega) \approx 64 \omega^4$. Numerical results are presented in the next section, where we analyze dissipation and decoherence in a harmonic potential well.

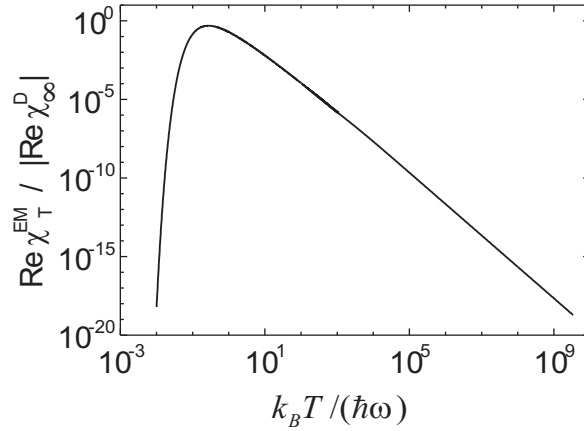


FIG. 3. Dispersive thermal susceptibility for the electromagnetic field. We plot $\text{Re } \chi_T^{\text{EM}} = \text{Re } \chi_{T!1}^{\text{D}}$ as a function of $k_B T = (\hbar \omega)$.

IV. DISSIPATION AND DECOHERENCE

In this section, we consider the effect of the quantum radiation pressure force on the motion of the mirror. We start with a classical description of the position of the mirror, and analyze the damping of the mirror's oscillation in a harmonic potential well (frequency ω_0). Later in this section we also consider the quantum dynamics of the mirror, in order to derive the decoherence rate induced by radiation pressure. The limiting cases of zero and high temperatures were considered in Refs. [19] and [20], respectively. The results of the previous section allow us to take arbitrary values of temperature.

The equation of motion reads

$$m \ddot{q}(t) = -m \omega_0^2 q(t) + \int_{-\infty}^{\infty} dt' \tilde{\gamma}(t-t') \dot{q}(t') ; \quad (28)$$

where $\tilde{\gamma}(t)$ denotes the inverse Fourier transform of $\gamma(\omega)$; with $\gamma(\omega) = \gamma^{\text{D}}(\omega)$ for the scalar field model and $\gamma(\omega) = \gamma^{\text{EM}}(\omega)$ for the electromagnetic case. Its solutions are of the form $q(t) = e^{i\omega_0 t} \tilde{q}$, where the complex constant \tilde{q} is found by replacing this function into (28):

$$m \omega^2 = -m \omega_0^2 + \gamma(\omega) : \quad (29)$$

We include the dispersive effect of the vacuum field through a renormalization of the bare mass and frequency of oscillation, so that m and ω_0 in (28) and (29) are already renormalized and ω in (29) is replaced by $\text{Re } \omega_T + i(\text{Im } \omega_{\text{vac}} + \text{Im } \omega_T)$: This allows us to assume that the effect generated by the radiation pressure force is a small perturbation of the free oscillations at frequency ω_0 when computing the roots of Eq. (29). Hence they are of the form $\omega = (\omega_0 + \omega_T) - i\gamma$; with $\gamma \propto \omega_T \omega_0$: γ is the damping rate, and ω_T is the frequency shift induced by the coupling with thermal photons. Using that $\text{Re } \omega_T$ ($\text{Im } \omega$) is an even (odd) function of γ ; we find from (29)

$$\omega_T = \frac{\text{Re } \omega_T(\omega_0)}{2m\omega_0} \quad (30)$$

and

$$\gamma = \frac{\text{Im } \omega(\omega_0)}{2m\omega_0}; \quad (31)$$

The case of a mass correction δm provides a trivial application of (30) (this is the case for the 3D scalar field for frequencies much smaller than $k_B T = \hbar$; but not for the electromagnetic field): when the dispersive susceptibility is of the form $\text{Re } \chi_T(\omega) = m_p \omega^{-2}$; (30) yields $\omega_T = \omega_0 = m = (2m)$; which is just the first order expansion of the exact result $(\omega_0 + \omega_T) = \omega_0 = m/(m + \delta m)$:

As discussed in Sec. II, $\text{Im } \omega(\omega_0)$ is always positive since energy is taken from (and not given to) the mirror; hence γ ; as given by (31), is positive, which corresponds to exponential decay as required.

Of particular interest is the application of (31) to the electromagnetic case, which we analyze in the rest of this section. At zero temperature, Eqs. (24) and (31) yield (here and in the next section we re-introduce the speed of light c)

$$\gamma_{\text{vac}} = \frac{1}{30} \frac{\hbar \omega_0}{2m c^2} \frac{A \omega_0^2}{c^2} \omega_0; \quad (32)$$

Hence γ_{vac} is proportional to the ratio between the zero point and the rest mass energies of the mirror. Despite of the geometrical factor $A \omega_0^2 = c^2$; representing the squared ratio between the transverse size of the mirror and the typical vacuum field wavelength (for frequencies in the GHz range $c = \omega_0$ is in the centimeter range), we have $\gamma_{\text{vac}} \ll \omega_0$; as required for consistency of the derivation.

In the high-temperature limit, Eq. (31) yields

$$\gamma_{\text{th}} = \frac{2}{15} \frac{k_B T}{m c^2} \frac{A}{c^2} \frac{k_B T}{\hbar}; \quad (33)$$

in agreement with Ref. [20]. Except for a numerical factor, (33) differs from (32) by the replacement of the zero point energy $\hbar \omega_0/2$ by $k_B T$ and the frequency scale ω_0 by $k_B T = \hbar$: In Fig. 4, we plot

$$\frac{\gamma_{\text{vac}}}{\gamma_{\text{th}}} = 1 + \frac{\text{Im } \chi_T^{\text{EM}}}{\text{Im } \chi_{\text{vac}}^{\text{EM}}} = 1 + \frac{1}{12} G^{\text{EM}} \frac{k_B T}{\hbar \omega_0}$$

as a function of $k_B T = (\hbar \omega_0)$ (solid line), showing the T^4 behavior corresponding to the high-temperature approximation as given by Eq. (33), which is only 4% larger than the numerical exact value at $k_B T = (\hbar \omega_0) = 1$:

In order to analyze the effect of decoherence, we now consider the quantum dynamics of the mirror in the potential well. We assume that the mirror state is initially a coherent superposition of two coherent states: $|j\rangle = (|j_0\rangle + |j_0 + 1\rangle)/\sqrt{2}$; with

$$j_0 = \frac{1}{4} \frac{Z}{Z_0} \ll 1;$$

where Z represents the distance between the wavepacket components at $t = 0$; and $Z_0 = \sqrt{\hbar/2m\omega_0}$ is the uncertainty of position of the ground state.

The free evolution preserves the form (and the coherence) of the initial state, with j_0 replaced by $j(t) = j_0 \exp(-i\omega_0 t)$: The very weak radiation pressure coupling with the field introduces two new time scales, both assumed to be much larger than the free evolution time scale $2\pi/\omega_0$: The time needed to reach thermal equilibrium is the largest time scale. At zero temperature, it corresponds to $1/\gamma$ (2); where γ is the amplitude damping rate discussed before in the classical theory. In fact, in this particular case, the equilibrium state is of course the ground state of the harmonic oscillator. During the decay process, the energy quantity $(2j_0^2 - 1)\hbar\omega_0$ is dissipated by the

dynamical Casimir effect, with the emission of about $2 \frac{\hbar \omega_0}{2}$ pairs of photons, since the energy contained in each pair is $\hbar \omega_0$ [13]–[15] [21].

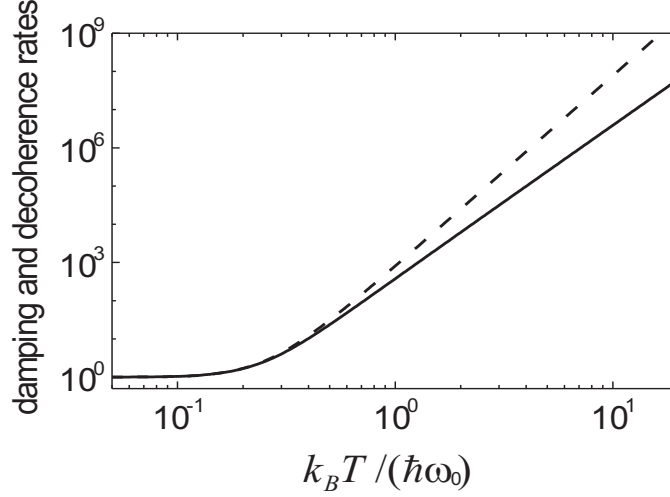


FIG. 4. Damping and decoherence rates for a mirror in a harmonic potential well. We plot γ_{vac} (solid line) and γ_{vac}^{dec} (dashed line) as functions of $k_B T / (\hbar \omega_0)$. Results for the damping and decoherence rates at zero temperature γ_{vac} and γ_{vac}^{dec} are discussed in the text; note that $\gamma_{vac}^{dec} = \gamma_{vac}$.

The second time scale corresponds to the process of decoherence. The state decays into the incoherent statistical mixture $\rho = \frac{1}{2}(|j\rangle\langle j| + |j+1\rangle\langle j+1|)$ much before reaching thermal equilibrium. The decoherence time is much shorter than the damping time because a single photon pair already contains ‘which way’ information sufficient to destroy the possibility of interference between the two components. Since the time scale corresponding to the emission of $2 \frac{\hbar \omega_0}{2}$ pairs is $1/(2\gamma)$; the decoherence time at zero temperature is $1/(4\gamma) = 1/(4\gamma_{vac})$ (see [20]). The decoherence rate γ^{dec} is defined as the inverse of the corresponding time scale. Assuming $\gamma^{dec} = 4\gamma$; Ref. [20] derives a relation between decoherence and damping rates valid for arbitrary values of temperature:

$$\gamma^{dec} = \frac{1}{4} \coth\left(\frac{\hbar \omega_0}{2k_B T}\right) \left(\frac{Z}{Z_0}\right)^2 : \quad (34)$$

Formally, the factor $\coth(\hbar \omega_0 / 2k_B T)$ originates from the fluctuation-dissipation theorem, since decoherence may be described as a process of diffusion in phase space, which washes out the interference oscillations characterizing the coherence of the superposition state [22]. At high temperatures, this factor is approximately $2k_B T / (\hbar \omega_0)$; jointly with the high-temperature behavior of γ ; it results in T^5 dependence. This power law, also obtained in Ref. [23] in the case of a free particle, is visible in Fig. 4 (dashed line), where we plot $\gamma^{dec} = \gamma_{vac}^{dec} = \coth(\frac{\hbar \omega_0}{2k_B T}) \gamma_{vac}$ as a function of $k_B T / (\hbar \omega_0)$. Both γ and γ^{dec} are already one order of magnitude larger than the vacuum values for $k_B T / (\hbar \omega_0) \approx 0.4$; showing that the thermal effect dominates even for moderate values of temperature.

According to (34), decoherence is faster the larger is the separation Z between the wave packets. For large separations, ‘which way’ information is more readily available since the two state components are better resolved, as compared to their widths in phase space. At zero temperature, zero-point fluctuations define the corresponding scale of length Z_0 : In the high-temperature limit, on the other hand, the additional factor $2k_B T / (\hbar \omega_0)$ in (34) yields $\gamma^{dec} = (Z/Z_T)^2 \gamma_{vac}$; the thermal de Broglie wavelength $\lambda_T = h / \sqrt{2m k_B T}$ replacing Z_0 as the reference of length scale.

In conclusion, coherent superpositions of states very far apart in phase space are extremely unstable, since they decay into the corresponding statistical mixtures in a very short time. In the opposite extreme, coherent states are the most stable ones, in the sense that they generate the least entropy when interacting with the field [20]. They correspond to the ‘pointer states’, which play an important role in the classical limit of quantum mechanics [24]. Here we have discussed a particular physical mechanism of decoherence, which illustrates some of its general properties. The corresponding orders of magnitude are discussed in the end of the next section.

The temperature of the field defines the frequency scale $k_B T = \hbar$: The motion is slow when the mechanical frequencies satisfy $\omega \ll k_B T = \hbar$: Hence the quasi-static regime corresponds to the high temperature limit. We summarize below the results obtained for this regime, now taking the time domain.

For the scalar field, we have found

$$F^D(t) = \frac{2}{15} \frac{(k_B T)^4}{\hbar^3 c^4} A \dot{q}(t) + \frac{(3)}{2} \frac{(k_B T)^3}{\hbar^2 c^4} A \ddot{q}(t): \quad (35)$$

The dissipative force results, in general, from input modes corresponding to regions R_1 ; R_2 and R_3 in Fig. 1. R_3 corresponds to the input modes involved in the process of photon creation. At zero temperature, only R_3 contributes, whereas in the quasi-static (high temperature) limit R_1 and R_2 provide the dominant contribution as shown in Appendix B. Thus, the dissipative component in (35) (1st term in its r.h.s.) originates from scattering of thermal photons, rather than from creation of photons. It is of the form [25] $2P_T = c^2 \dot{q}(t)$; where P_T representing the total power incident on (both sides of) the mirror, is proportional to T^4 as predicted by the Stefan-Boltzmann law. This viscous force results from Doppler shifting the reflected thermal photons [9].

The dispersive component also appearing in (35) corresponds to a temperature-dependent, finite, and very small mass correction

$$m = \frac{(3)}{2} \frac{(k_B T)^3}{\hbar^2 c^4} A: \quad (36)$$

For $T = 300K$; we find $m = A \cdot 1.5 \cdot 10^{-29} g = cm^2$: m results from the contribution of input propagating modes that are scattered into evanescent waves (region R_4 in Fig. 1). It corrects the (experimentally known) zero-temperature mass of the mirror, which already contains the mass renormalization generated by vacuum fluctuations [14]–[16]. Even at zero temperature, the mass is modified when a second plate is present [26] [27], or if its surface is corrugated [28]. In all three cases, the mass correction is a finite measurable quantity that depends on some control parameter: temperature, distance between the plates, or amplitude of corrugation.

For the electromagnetic field, the viscous force is twice as large as in the scalar case, the two polarizations providing identical contributions:

$$F^{EM}(t) = \frac{2}{15} \frac{(k_B T)^4}{\hbar^3 c^4} A \dot{q}(t): \quad (37)$$

Eq. (37) agrees with Ref. [20], where the force is derived by considering the Doppler shift of the thermal photons. For $T = 300K$; the pressure is $4.1 \cdot 10^{-14} N/m^2$ for a velocity of $1m/s$:

For the dispersive force, on the other hand, the contributions from the two field polarizations cancel, as discussed in Sec. III, and the quasi-static force as given by (37) does not contain a term proportional to the second-order time derivative. Thus, in contrast to the scalar case, the mass correction vanishes in the electromagnetic case (it also vanishes for a scalar field in one dimension [9]). This difference between the two models is better understood by considering the thermodynamics of the field at temperature T in the presence of a static mirror. In Appendix C, we compute the Helmholtz free energy

$$F = -k_B T \ln Z; \quad (38)$$

where Z is the partition function, for both models. For the scalar field, the free energy in a volume V is $F^D = E_{vac}^D + F_T^D$; where E_{vac}^D is the zero-point energy, and

$$F_T^D = \frac{2}{90} \frac{(k_B T)^4}{(\hbar c)^3} V + \frac{(3)}{4} \frac{(k_B T)^3}{(\hbar c)^2} A: \quad (39)$$

The 1st term in (39) is the free-space thermal free energy, featuring the characteristic T^4 power law. For us, the interesting term is the second one. It is an effect of the Dirichlet boundary condition at the mirror's surface, which eliminates field modes propagating along directions parallel to the mirror. In fact, this term is not present in the electromagnetic case:

$$F_T^{EM} = \frac{2}{45} \frac{(k_B T)^4}{(\hbar c)^3} V; \quad (40)$$

because of the contribution from TM-polarized grazing eld modes (whereas the free-space term is twice the scalar result due to the equal contributions from the two orthogonal polarizations).

From (39) and (40) we may also compute the entropy $S = -\partial F/\partial T = -\partial F_T/\partial T$ and the internal energy $U = F + TS$: For the scalar eld, we find $U^D = E_{vac}^D + U_T^D$; with

$$U_T^D = \frac{2}{30} \frac{(\kappa_B T)^4}{(hc)^3} V + U_T; \quad (41)$$

and $U_T = -\pi^2/15 (hc)^{-3}$: U_T represents the difference between the thermal energies in the presence of the static mirror and in free space. As discussed in Appendix D, where we present an alternative, 'local' derivation of U_T^D ; the energy density is decreased significantly (with respect to its free-space value) over a distance from the mirror of the order of $hc/\kappa_B T$:

For the electromagnetic eld, on the other hand, both F_T^{EM} and U_T^{EM} are not modified by the mirror according to (40) (this may also be inferred from the result of Ref. [29] for a two-plates configuration by taking the limit of large separation), and consistently the mass correction vanishes in this case.

In the low temperature (or high mechanical frequency) limit, thermal photons provide a small correction of the vacuum dissipative force, of the order of $(\kappa_B T/\hbar)^4$; whereas the thermal dispersive correction is exponentially small, for both scalar and electromagnetic cases. We have also presented numerical results for arbitrary values of temperature, allowing us to discuss damping and decoherence of a mirror in a harmonic potential well in this general case. For both effects, thermal fluctuations dominate over zero-point fluctuations for temperatures above $0.3\hbar/\kappa_B$; and the high temperature approximation provides accurate values for temperatures above \hbar/κ_B : Although the effect of damping of energy is usually negligible, thermal radiation pressure efficiently destroys the coherence of a quantum superposition state. For $T = 300K$ and $A = 1\text{cm}^2$; the decoherence time is $\tau_{dec} = 1.3 \times 10^{-12}\text{s}$ when the distance between the wave packet components is only $Z = 1\text{nm}$ [30].

ACKNOWLEDGMENTS

P.A.M.N. thanks D. Dalvit, A. Lambrecht and S. Reynaud for discussions, and PRONEX, FAPERJ and the Millennium Institute of Quantum Information for financial support. C.F. and P.A.M.N. thank CNPq for partial financial support.

APPENDIX A: DISPERSIVE THERMAL SUSCEPTIBILITY

As discussed in Sec. II, the dispersive thermal susceptibility $\text{Re } \chi_T^D(\omega)$ is given by the term proportional to \bar{n} in Eq. (15), to be integrated over the region R_4 in Fig. 1 (for the sake of clarity we assume $\omega > 0$ in the derivation so as to be able to refer to Fig. 1):

$$\text{Re } \chi_T^D(\omega) = \frac{\hbar A}{2} \int_{R_4} d\omega_{in} dk_k k_k \frac{q}{k_k^2} \frac{q}{(\omega + \omega_{in})^2} \frac{1}{\omega_{in}^2} \frac{1}{k_k^2} \bar{n}(\omega_{in}) \quad (A1)$$

Eq. (A1) shows that $\text{Re } \chi_T^D(\omega) < 0$ for any ω : We change to the variables

$$u = \frac{\hbar(\kappa_k - \omega_{in})}{\kappa_B T}; \quad v = \frac{\hbar(\kappa_k + \omega_{in})}{\kappa_B T}; \quad (A2)$$

The Jacobian for this transformation yields

$$|J| = \frac{\partial(u,v)}{\partial(\kappa_k; \omega_{in})} = 2 \frac{\hbar}{\kappa_B T}; \quad (A3)$$

From (A1) and (A3) we find

$$\text{Re } \chi_T^D(\omega) = \frac{\hbar A}{4} \frac{\kappa_B T}{h} \int_0^{\omega} dv \int_{\omega-v}^{\omega+v} du (u-v) \frac{e^{-\frac{u+v}{2}}}{1 - e^{-\frac{u+v}{2}}}; \quad (A4)$$

where $\omega = \hbar/(\kappa_B T)$: We use (A4) to calculate $\text{Re } \chi_T^D(\omega)$ numerically (see figure 2). Because of the exponential factor, the dominant contribution comes from values $u < 1$: In the high-temperature approximation, $\omega \ll 1$; we have

v and u : Hence we may neglect v^2 and v inside the root and v in the exponential in (A 4), and replace the lower limit of integration over u by zero. We get

$$\operatorname{Re} \epsilon_T^{(D)}(\omega) = \frac{\hbar A}{4^2} \frac{k_B T}{h} \int_0^{\omega} dv \int_0^{\omega-v} du \frac{u^2}{e^{\frac{u}{2}}} + O(\omega^{-2}) \quad (\text{A } 5)$$

The remaining integrals in (A 5) give $\frac{1}{2} \ln 2$; yielding the result of (18).

In the low temperature limit, $\omega \gg 1$; we may approximate the average photon number as follows:

$$f_{\text{exp}}[(u+v)=2] \approx \frac{1}{2} e^{-2};$$

because $(u+v)=2$ is the dominant contribution in (A 4). We change to new variables s and t with $v = s^2$ and $u = 1 + t^2$ and integrate over t by parts to find

$$\operatorname{Re} \epsilon_T^{(D)}(\omega) = \frac{\hbar A}{4^2} \frac{k_B T}{h} \int_0^{\omega} ds s^2 \int_0^{\omega-s^2} dt \frac{e^{-\frac{1+t^2}{2}}}{1+t^2} (1+t^2)^{-\frac{1}{2}} e^{-s^2} = \frac{\hbar A}{4^2} \frac{k_B T}{h} \int_0^{\omega} ds s^2 \int_0^{\omega-s^2} dt \frac{e^{-\frac{1+t^2}{2}}}{1+t^2} (1+t^2)^{-\frac{1}{2}} e^{-s^2} \quad (\text{A } 6)$$

The integral over t gives $\frac{1}{2} \ln 2 = \frac{1}{2} \ln(1+s^2)$ by the method of steepest descent, the saddle point $t = 0$ corresponding to the condition $k_k = \omega_{\text{in}} = \omega$: The resulting integral over s is also calculated by first integrating by parts, and then using the steepest descent method. The saddle point is at $s = 0$; corresponding to $\omega_{\text{in}} = k_k$: Thus, the dominant contribution in (A 1) comes from the close neighborhood of $k_k = \omega_{\text{in}} = \omega$; which corresponds to nearly grazing modes, and the final expression is given by (17).

As discussed in Sec. III, the contribution of TE-polarized modes to the electromagnetic susceptibility turns out to be identical to $\epsilon_T^{(D)}$: The TM contribution is given by the r.h.s. of (23), its real T-dependent part yielding

$$\operatorname{Re} \epsilon_T^{(TM)}(\omega) = \frac{\hbar A}{4^2} \frac{k_B T}{h} \int_0^{\omega} dv \int_0^{\omega-v} du \frac{u}{e^{\frac{u+v}{2}}} \frac{v}{1+uv} \frac{(u+v)^2}{(u-v)}; \quad (\text{A } 7)$$

It is clear from this equation that $\operatorname{Re} \epsilon_T^{(TM)}(\omega)$ is positive for any frequency ω : Using the same methods employed in the scalar case, we derive from this equation the limiting cases corresponding to high and low temperatures.

In the high-temperature limit, we derive from (A 7)

$$\operatorname{Re} \epsilon_T^{(TM)}(\omega) = \frac{\hbar A}{4^2} \frac{k_B T}{h} \int_0^{\omega} dv \int_0^{\omega-v} du \frac{u^2}{e^{\frac{u+v}{2}}} + O(\omega^{-2}); \quad (\text{A } 8)$$

The integrals above are readily calculated, resulting in (25).

In the low temperature limit, we change to the variables s and t employed in the derivation of the scalar susceptibility, and derive from (A 7)

$$\operatorname{Re} \epsilon_T^{(TM)}(\omega) = \frac{\hbar A}{4^2} \frac{k_B T}{h} \int_0^{\omega} ds s^2 \int_0^{\omega-s^2} dt \frac{e^{-\frac{1+t^2}{2}}}{1+t^2} \frac{s^2}{1+t^2} (1+t^2)^{-\frac{1}{2}} (s^2-1)^{-\frac{1}{2}} e^{-s^2} = \frac{\hbar A}{4^2} \frac{k_B T}{h} \int_0^{\omega} ds s^2 \int_0^{\omega-s^2} dt \frac{e^{-\frac{1+t^2}{2}}}{1+t^2} \frac{s^2}{1+t^2} (1+t^2)^{-\frac{1}{2}} (s^2-1)^{-\frac{1}{2}} e^{-s^2} \quad (\text{A } 9)$$

The integral over t gives $\frac{1}{2} \ln 2 = \frac{1}{2} \ln(1+s^2)^3 = \frac{3}{2} \ln(1+s^2)$ by the method of steepest descent (saddle point at $t = 0$). Then the integral over s is also computed with this method (saddle point at $s = 0$), yielding the result of (26). As in the scalar case, the dominant contribution comes from nearly grazing waves with frequencies close to $\omega_{\text{in}} = \omega$:

APPENDIX B: DISSIPATIVE THERMAL SUSCEPTIBILITY

We calculate $G^D(\omega)$; defined in (19), from (15), taking the imaginary part of the term proportional to \bar{n} : We change to the dimensionless variables $\omega_0 = \hbar \omega_{\text{in}} = (k_B T)$ and $K = \hbar k_k = (k_B T)$: For the contribution from region R_2 in Fig. 1, we also change ω_0 into ω_0' ; with $\omega_0' = \hbar \omega_{\text{in}} = (k_B T) = 1$: The joint contribution from R_1 and R_2 is given by

$$G_{(1+2)}^D(\omega) = 360^{-5} (e^{-\omega_0} - 1) \int_0^{\omega_0} d\omega_0' \int_0^{\omega_0'} dK K \frac{e^{-\frac{1}{2}(\omega_0'^2 - K^2)} [(1 + \omega_0'^2) - K^2] e^{-\frac{1}{2}(\omega_0'^2 - K^2)}}{(e^{-\omega_0'} - 1)(e^{-\omega_0} - 1)}; \quad (\text{B } 1)$$

We split region R_3 into two sub-regions, corresponding to the intervals $\omega_0' = \omega_{\text{in}} = \omega$; and $\omega_0' = \omega_{\text{in}} = 0$: We change ω_0' into $\omega_0' + \omega_0$ when integrating over the first sub-region, and into ω_0' for the second sub-region. We find

$$G_{(3)}^D(\omega) = 360 \int_0^{\omega} d\omega' \int_0^{\omega'} dK \frac{1}{(\omega^2 - K^2) [(\omega')^2 - K^2]} \left(\frac{1}{e^{\beta\omega'} - 1} + \frac{1}{e^{\beta\omega} - 1} \right); \quad (B2)$$

In the high-temperature limit, $\beta \rightarrow 0$; we take $e^{\beta\omega} \approx 1$ and neglect ω' in the integrand in (B1). We find $G_{(1+2)}^D(\omega) = 24 \int_0^{\omega} d\omega'$. For the evaluation of $G_{(3)}^D$, we take $1 = (e^{\beta\omega'} - 1)^{-1} \approx \beta\omega'$ [and likewise for $1 = (e^{\beta\omega} - 1)^{-1}$] in (B2) since ω' is bounded by ω . The final result is $O(\omega)$ and can be neglected. This completes the derivation of the high-temperature limit of $G^D(\omega)$:

In the low-temperature limit, $\beta \rightarrow \infty$; we replace $1 = (e^{\beta\omega'} - 1)^{-1}$ by $e^{-\beta\omega'}$; canceling the exponential factors in the numerator in (B1). Actually, this is equivalent to neglect the contribution from R_2 : In fact, in this approximation only the close neighborhood of the origin in Fig. 1 contributes (as discussed in Appendix A, the dispersive component is exponentially small by a similar reason, since it results from region R_4 , which is far from the origin). We also take $\frac{1}{(\omega')^2 - K^2} \approx \frac{1}{\omega'^2}$ in (B1) and (B2), and in (B2) neglect $1 = (e^{\beta\omega} - 1)^{-1}$ and replace the upper bound of the integral over ω' by infinity. In this approximation, the contributions from R_1 and R_3 are equal, and we find

$$G_{(1+2)}^D(\omega) = G_{(3)}^D(\omega) = 120 \int_0^{\omega} d\omega' \frac{\omega'}{e^{\beta\omega'} - 1}; \quad (B3)$$

The remaining integral in (B3) gives $\int_0^{\omega} \frac{\omega'}{e^{\beta\omega'} - 1} d\omega' = 15$; completing the derivation of the low-temperature limit of $G^D(\omega)$:

In order to derive the dissipative susceptibility for the electromagnetic field, we need to consider the contribution of TM-polarized modes, which is given by the T -dependent imaginary part of the expression given by (23). The contributions from R_1 and R_2 give

$$G_{(1+2)}^{(TM)}(\omega) = 360 \int_0^{\omega} d\omega' \int_0^{\omega'} dK \frac{K}{(\omega^2 - K^2) [(\omega')^2 - K^2]} \frac{e^{-\beta\omega'}}{(e^{\beta\omega'} - 1)(e^{\beta\omega} - 1)}; \quad (B4)$$

whereas the contribution from R_3 gives

$$G_{(3)}^{(TM)}(\omega) = 360 \int_0^{\omega} d\omega' \int_0^{\omega'} dK \frac{K}{(\omega^2 - K^2) [(\omega')^2 - K^2]} \left(\frac{1}{e^{\beta\omega'} - 1} + \frac{1}{e^{\beta\omega} - 1} \right); \quad (B5)$$

In the high-temperature limit, the contribution from Region R_3 is $O(\omega)$ and hence negligible as in the scalar case, whereas the contribution from R_1 and R_2 is derived from (B4) by neglecting ω' in the integrand and by taking $e^{\beta\omega} \approx 1$: We find $G_{(1+2)}^{(TM)}(\omega) = G^{(TE)}(\omega) \equiv G^D(\omega)$:

For low temperatures, we proceed as in the discussion of the scalar case: the contributions from R_1 and R_3 are identical, and from R_2 negligible. We find $G_{(1+2)}^{(TM)}(\omega) = 48 \int_0^{\omega} d\omega'$. When added to $G^{(TE)}(\omega) = 16 \int_0^{\omega} d\omega'$, we get the electromagnetic result as discussed in Sec. III.

APPENDIX C: FIELD FREE ENERGY WITH A STATIC MIRROR

We discuss both scalar (with Dirichlet boundary conditions) and electromagnetic field models. We first consider two parallel mirrors at rest separated by a distance L ; and compute the free energy in the volume $V = AL$ contained within the mirrors. Then, we take the limit $L \rightarrow \infty$ so as to identify the single-mirror effect. In this limit, we find a term proportional to V ; corresponding to the free-space case, and, in the scalar case, a term proportional to A ; which does not depend on L : The latter contains the independent single-mirror effects of the two mirrors, with only one side of each mirror taken into account. By symmetry, this is equal to the effect of one mirror when both sides are taken into account. The free energy for two parallel plates has been calculated by several different methods [31]. Here we follow the approach of Ref. [32].

The partition function is defined as

$$Z = \text{tr} \exp[-H_0/(k_B T)]; \quad (C1)$$

with $H_0 = \sum_{\mathbf{k}} \hbar \omega_{\mathbf{k}} (a_{\mathbf{k}}^\dagger a_{\mathbf{k}} + 1/2)$; $\{\omega_{\mathbf{k}}\}$ represents a set of parameters defining a given field mode (which also contains an index for polarization in the electromagnetic case), with $\omega_{\mathbf{k}} = \frac{c}{L} \sqrt{(n\pi)^2 + k_\perp^2}$. Eq. (C1) yields

$$Z = \frac{e^{-\hbar/2k_B T}}{1 - e^{-\hbar/(k_B T)}}; \quad (C2)$$

which combined with (38) leads to

$$F = \sum_{n=0}^{\infty} \frac{\hbar \omega_n}{2} + k_B T \sum_{n=0}^{\infty} \ln \left(1 - e^{-\hbar \omega_n / (k_B T)} \right) \quad (C 3)$$

The first term in (C 3) represents the zero point energy E_{vac} . We want to compute the second term, which contains the temperature dependence:

$$F_T = \sum_{n=0}^{\infty} g(n) a(n); \quad (C 4)$$

where

$$a(n) = \frac{A k_B T}{2} \int_0^{\infty} dk_k k_k \ln \left(1 - \exp \left[- \frac{\hbar \sqrt{(n\pi/L)^2 + k_k^2}}{k_B T} \right] \right); \quad (C 5)$$

with $g(n) = 1$ for $n=0$ and $g(n) = 2$ for $n>0$ in the scalar and electromagnetic models, respectively. Hence in the former case grazing modes, corresponding to $n=0$, are ruled out, whereas in the electromagnetic model TM polarized grazing modes provide a non vanishing contribution to the free energy.

In order to compute F_T , we employ Poisson sum formula

$$\frac{1}{2} a(0) + \sum_{n=1}^{\infty} a(n) = A_0 + 2 \sum_{j=1}^{\infty} \text{Re} A_j; \quad (C 6)$$

where

$$A_j = \int_0^{\infty} dk_k a(n) e^{i 2 j n}; \quad (C 7)$$

We change the variable of integration from k_k to $\hbar \sqrt{(n\pi/L)^2 + k_k^2} = (k_B T)$; and integrate over n to find

$$A_0 = \frac{2 V (k_B T)^4}{90 \hbar^3}; \quad (C 8)$$

and for non vanishing values of j ;

$$A_j = \frac{A (k_B T)^3}{2^2 j \hbar^2} \int_0^{\infty} d \ln(1 - e^{-x}) \frac{e^{i j x}}{2i}; \quad (C 9)$$

where $j = 2 j L k_B T / \hbar$. By integrating the r.h.s. of (C 9) by parts, we find

$$\text{Re} A_j = \frac{A (k_B T)^2}{8^2 j^2 \hbar L} \left(\frac{1}{2^2 j} \left[j \coth \left(\frac{1}{j} \right) - 1 \right] + \text{Re} \int_0^{\infty} d \frac{e^{i j x}}{1 - e^{-x}} \right); \quad (C 10)$$

We calculate the r.h.s. of (C 10) in the limit $j \rightarrow \infty$: By successive integrations by parts, one may show that the last term within brackets in (C 10) yields $1/(2^2 j) + O(1/j^3)$ and may be neglected in (C 10):

$$\text{Re} A_j = \frac{A k_B T}{32^2 j^3 L^2} [1 + O(1/j)]; \quad (C 11)$$

Hence in the limit $L \rightarrow \infty$ only A_0 contributes in the Poisson sum formula Eq. (C 6).

Finally, when computing the free energy for the scalar Dirichlet field, we need to subtract $a(0)=2$ from the r.h.s. of (C 6), since $g(0) = 0$ in (C 4) in this case. We calculate $a(0)$ from (C 5):

$$a(0) = \frac{(3) A (k_B T)^3}{2 \hbar^3}; \quad (C 12)$$

Combining (C 4), (C 6), (C 8) and (C 12), we derive the free energy for the Dirichlet field and a single static plate as given by (39). For the electromagnetic field, on the other hand, we may employ Poisson formula directly, since in this case the sum over n in (C 4) has already the form of the l.h.s. of (C 6). Then we find $F_T^{EM} = 2 A_0$ [with A_0 given by (C 8)], in agreement with (40).

In this appendix, we compute the energy density

$$w(z) = \frac{1}{2} h(\partial_t)^2 + (r)^2 i \quad (D 1)$$

for a scalar field at temperature T ; and with Dirichlet boundary conditions at $z = 0$: Since we consider the static case, we replace ∂_t by ∂_z ; and from its normal mode expansion as given by Eq. (7) derive (with $k = \sqrt{k_x^2 + k_z^2}$)

$$w(z) = \frac{h}{2} \int_0^\infty dk_z \int_0^\infty dk_k \frac{k_k}{k} h(k^2 + k_k^2 \sin^2(k_z z) + k_z^2 \cos^2(k_z z)) \frac{1}{2} + \bar{n}(k) : \quad (D 2)$$

As in the derivation of the susceptibility (!); the energy density is naturally split into two contributions, one from vacuum fluctuations [the '1=2' inside brackets in (D 2)], the other from thermal fluctuations, which corresponds to the factor $\bar{n}(k)$ in (D 2). Accordingly, we write $w = w_T + w_{vac}$: Here we are only interested in the thermal contribution w_T ; which is obtained from (D 2) after changing the variable of integration from k_k to k :

$$w_T(z) = \frac{2}{30} \frac{(k_B T)^4}{h^3} + w_T : \quad (D 3)$$

The first term in (D 3) represents the free-space energy density for a scalar field; the effect of the boundary at $z = 0$ is contained in w_T :

$$w_T(z) = \frac{h}{8} \frac{1}{z^2} - \frac{k_B T}{2 h z^3} \coth \frac{2 k_B T z}{h} - \frac{k_B T}{h z} \frac{1}{\sinh^2 \frac{2 k_B T z}{h}} : \quad (D 4)$$

$w_T(z)$ is a negative-defined, increasing function of z that goes to zero as $kT = (16/z^2)$ for $z = h/(k_B T)$: Hence the mirror reduces the thermal energy density, an effect stronger near the mirror. w_T is finite at $z = 0$; and vanishes at $T = 0$ as expected from its definition.

The total modification of the internal energy is given by the volume integral of $w_T(z)$; taking into account both sides of the mirror:

$$U_T = 2A \int_0^\infty dz w_T(z) = \frac{A}{4} \frac{(k_B T)^3}{h^2} \int_1^\infty dZ \frac{2}{Z^4} - \frac{\coth Z}{Z^3} - \frac{1}{Z^2 \sinh^2 Z} : \quad (D 5)$$

The integral above may be computed with the method of residues, by taking a semi-circular path (radius $\rightarrow \infty$) in the complex plane of Z : The poles of the integrand lie along the imaginary axis, at the positions $Z = in$; with n integer, $n \neq 0$: We find

$$U_T = \frac{1}{2} A \frac{(k_B T)^3}{h^2} \sum_{n=1}^\infty \frac{1}{n^3} : \quad (D 6)$$

The series appearing in (D 6) is equal to (3): Then, comparing (36) with (D 6), we find $U_T = \frac{1}{2} m c^2$ as discussed in Sec. V.

- [1] H. B. G. Casimir, Proc. K. Ned. Akad. Wet. 51, 793 (1948).
- [2] G. Barton, J. Phys. (London) A : Math. Gen. 24, 5533 (1991); C. Eberlein, ibid. 25, 3015 (1992).
- [3] V. B. Braginsky and F. Ya. Khalili, Phys. Lett. A 161, 197 (1991); M. T. Jaekel and S. Reynaud, Quantum Opt. 4, 39 (1992).
- [4] G. T. Moore, J. Math. Phys. 11, 2679 (1970).
- [5] S. A. Fulling and P. C. W. Davies, Proc. R. Soc. London A 348, 393 (1976).
- [6] L. H. Ford and A. Vilenkin, Phys. Rev. D 25, 2569 (1982).

- [7] P. A. M. Maia Neto, J. Phys. A 27, 2167 (1994).
- [8] G. Barton, New aspects of the Casimir effect: fluctuations and radiative reaction, in Cavity Quantum Electrodynamics, Supplement: Advances in Atomic, Molecular and Optical Physics, edited by P. Bernan (Academic Press, New York, 1993); P. A. M. Maia Neto and S. Reynaud, Phys. Rev. A 47, 1639 (1993).
- [9] M. T. Jaekel and S. Reynaud, Phys. Lett. A 172, 319 (1993).
- [10] A. Lambrecht, M. T. Jaekel and S. Reynaud, Europhys. Lett. 43, 147 (1998); G. Plunien, R. Schutzhold and G. So, Phys. Rev. Lett. 84, 1882 (2000); J. Hui, S. Qing-Yun and W. Jian-Sheng, Phys. Lett. A 268, 174 (2000); R. Schutzhold, G. Plunien and G. So, Phys. Rev. A 65, 043820 (2002).
- [11] H. B. Callen and T. A. Welton, Phys. Rev. 83, 34 (1951); R. Kubo, Rep. Prog. Phys. 29, 255 (1966).
- [12] V. V. Dodonov, A. B. Klimov and V. I. Man'ko, Phys. Lett. A 149, 225 (1990); P. A. M. Maia Neto and L. A. S. Machado, Brazilian J. Phys. 25, 324 (1995).
- [13] P. A. M. Maia Neto and L. A. S. Machado, Phys. Rev. A 54, 3420 (1996).
- [14] G. Barton and C. Eberlein, Ann. Phys. (N.Y.) 227, 222 (1993).
- [15] R. G. Unwin and C. Eberlein, J. Phys. (London) A: Math. Gen. 31, 6819 (1998).
- [16] G. Barton and A. Calogeracos, Ann. Phys. (N.Y.) 238, 227 (1995); A. Calogeracos and G. Barton, ibid. 238, 268 (1995).
- [17] M. Abramowitz and I. Stegun, Handbook of Mathematical Functions (Dover, New York, 1972).
- [18] D. F. M. Undarain and P. A. M. Maia Neto, Phys. Rev. A 57, 1379 (1998). Appendix A presents a detailed derivation of the boundary conditions.
- [19] D. A. R. Dalvit and P. A. M. Maia Neto, Phys. Rev. Lett. 84, 798 (2000).
- [20] P. A. M. Maia Neto and D. A. R. Dalvit, Phys. Rev. A 62, 042103 (2000).
- [21] A. Lambrecht, M. T. Jaekel and S. Reynaud, Phys. Rev. Lett. 77, 615 (1996).
- [22] For times much larger than $2\pi/\omega_0$; the diffusion coefficient $D(t)$ tends to an asymptotic constant value, which is related to the spectrum of fluctuations of the field taken at the particular frequency ω_0 : This allows us to employ the fluctuation-dissipation theorem and derive a simple relation between $D(t \rightarrow \infty)$ and the damping rate γ ; which results in (34). For consistency of the derivation, the decoherence time scale must be larger than $2\pi/\omega_0$: Thus, as in the discussion of damping, we are not allowed to consider the free particle limit ($\omega_0 = 0$). The limit of 'fast' decoherence (i.e., faster than the free evolution time scale) in the high temperature approximation was considered by Maia Neto and Dalvit [Decoherence effects of motion-induced radiation, in Modern challenges in quantum optics, edited by M. Oszag and J. C. Retamal (Springer, Berlin, 2001)]. In this case, the mirror does not have time to probe the potential well before decaying into an incoherent statistical mixture, and its effect is negligible as regards decoherence. The free particle case in the high temperature limit is also discussed in Ref. [23].
- [23] E. Joos and H. D. Zeh, Z. Phys. B 59, 223 (1985).
- [24] W. H. Zurek, S. Habib and J. P. Paz, Phys. Rev. Lett. 70, 1187 (1993).
- [25] V. B. Braginsky and A. B. Manukhin, Sov. Phys. JETP 25, 653 (1967); A. B. Matsko, E. A. Zubova and S. P. Vyatchanin, Optics Comm. 131, 107 (1996).
- [26] M. T. Jaekel and S. Reynaud, J. Phys. I (France) 3, 1093 (1993).
- [27] L. A. S. Machado and P. A. M. Maia Neto, Phys. Rev. D 65, 125005 (2002).
- [28] R. Golestanian and M. Kardar, Phys. Rev. Lett. 78, 3421 (1997); Phys. Rev. A 58, 1713 (1998).
- [29] L. S. Brown and G. J. Maclay, Phys. Rev. 184, 1272 (1969).
- [30] Remarkably, the mass dependence in [see (31)] is canceled by the mass introduced by Z_0 in (34), so that γ^{dec} does not depend on the mass of the mirror, for any T : Moreover, both γ and γ^{dec} do not depend on ω_0 in the high-temperature limit, provided that $\omega_0 \gg \gamma$; γ^{dec} (see [22]).
- [31] M. Fierz, Helv. Phys. Acta 33, 855 (1960); J. Mehra, Physica 37, 145 (1967); J. Ambjorn and S. Wolfram, Ann. Phys. NY 147, 1 (1983); N. F. Svaiter, Nuovo Cimento A 105, 959 (1992); M. V. Cougo-Pinto, C. Farina and A. Tort, Lett. Math. Phys. 37, 159 (1996).
- [32] G. Plunien, B. Muller and W. Greiner, Phys. Rep. 134, 88 (1986).